Dynamics of coupled repressilators: The role of mRNA kinetics and transcription cooperativity

I. Potapov, E. Volkov, and A. Kuznetsov

Phys. Rev. E **83**, 031901 — Published 4 March 2011

DOI: 10.1103/PhysRevE.83.031901

Dynamics of coupled repressilators: the role of mRNA kinetics and transcription cooperativity.

I. Potapov and E. Volkov
Department of Theoretical Physics, Lebedev Physical Inst., Leninskii 53, Moscow, Russia

A. Kuznetsov
Department of Mathematical Sciences and Center for Mathematical Biosciences, IUPUI, 402 N. Blackford St., Indianapolis, IN 46202, USA.

Oscillatory regulatory networks have been discovered in many cellular pathways. An especially challenging area is studying dynamics of cellular oscillators interacting with one another in a population. Synchronization is only one and simplest outcome of such interaction. It is suggested that the outcome depends on the structure of the network. A phase-attractive (synchronizing) and phase-repulsive coupling structures were distinguished for regulatory oscillators. In this paper, we question this separation. We study an example of two interacting repressilators (artificial regulatory oscillators based on cyclic repression). We show that changing the cooperativity of transcription repression (Hill coefficient) and reaction timescales dramatically alter synchronization properties. The network becomes birhythmic — it chooses between the in-phase and anti-phase synchronization. Thus, the type of synchronization is not characteristic for the network structure. However, we conclude that the specific scenario of emergence and stabilization of synchronous solutions is much more characteristic.

PACS numbers: 87.16.Yc, 05.45.-a, 87.18.-h

A. Introduction

Regulatory molecular networks are collections of interacting molecules in a cell. One particular kind, oscillatory networks, has been discovered in many pathways. Well-known examples are the circadian clock [1] and the cell cycle [2], where the oscillatory nature of the process plays a central role. Abnormalities of these processes lead to various diseases, from sleep disorders to cancer [3, 4]. For this reason, the regulatory oscillators attract significant attention among biologists and biophysicists.

These natural regulatory networks are very complex and include many types of molecules, from genes to small messengers. It is necessary to study the regulatory mechanisms by means of highly simplified models. These models are particularly valuable because *artificial* regulatory networks can be engineered experimentally [5–11]. The qualitative agreement between models and experiments is remarkable and validates the mathematical approach to the analysis of regulatory networks. Our goal is revealing general principles of cellular regulation by studying various artificial networks.

Modeling studies suggest several designs for artificial oscillatory networks. There are different implementations of hysteresis-based oscillators, [5, 9, 12, 13]. Another artificial oscillatory network called the repressilator [7] borrows the idea of a ring oscillator coming from engineering. Our computational study [14] suggests that the oscillatory mechanism of the repressilator is qualitatively different from that in other genetic oscillators.

A challenging area of the research is communication among cells in a population or organism. It is proposed to serve multiple very important functions from quorum sensing to differentiation [16]. In many cases, mechanisms of this intercell communication remain unknown. Artificial communication among cells containing regulatory oscillators can lead to various effects from synchronization to suppression of oscillations [13, 15, 17, 18]. These collective dynamical effects further contrasted artificial regulatory oscillators different by the design. A homogeneous population composed of repressilators, along with some other networks, was shown to display robust in-phase synchronization [15, 17, 19]. The property was regarded as a characteristic of the regulatory structure that they have in common. Accordingly, the coupling structure was called phase-attractive as opposed to the phase-repulsive that leads to the anti-phase synchronization [18]. In this paper, we question that the in-phase synchrony is the only option in such systems. We show that changing timescales and transcription cooperativity may dramatically alter synchronization properties and lead to other interesting dynamical effects in the network.

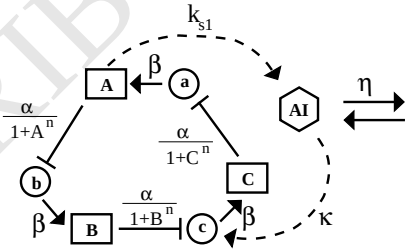

FIG. 1: The minimal scheme of repressilator with AI production [15].

The idea for the oscillatory mechanism of the repressilator is based on connecting an odd number of inverters (negative control elements) in a ring. Its genetic imple-

mentation uses three proteins that cyclically repress the synthesis of one another by inhibition of corresponding mRNA production (Fig. 1). A small molecule, autoinducer (AI), carries out the coupling function which is based on quorum sensing [15, 17]. The following system of dimensionless equations describes the behavior of coupled repressilators [15]:

$$\frac{da_i}{dt} = -a_i + \frac{\alpha}{1+C_i^n}; \qquad \frac{dA_i}{dt} = -\beta(A_i - a_i)$$

$$\frac{db_i}{dt} = -b_i + \frac{\alpha}{1+A_i^n}; \qquad \frac{dB_i}{dt} = -\beta(B_i - b_i)$$

$$\frac{dc_i}{dt} = -c_i + \frac{\alpha}{1+B_i^n} + \kappa\frac{S_i}{1+S_i}; \qquad \frac{dC_i}{dt} = -\beta(C_i - c_i)$$

$$\frac{dS_i}{dt} = -k_{s0}S_i + k_{s1}A_i - \eta(S_i - Q\bar{S})$$

The uppercase letters A_i, B_i and C_i denote protein concentrations, while lowercase a_i, b_i and c_i are proportional to the concentrations of mRNA corresponding to those proteins, S_i denotes AI concentration, where i is a cell index. $\bar{S} = \frac{1}{N}\sum_{i=1}^{N} S_i$, where N is the total number of cells; $N = 2$ in this work. All negative terms in the right-hand side represent degradation of the molecules. The nonlinear function $f(x) = \frac{\alpha}{1+x^n}$ reflects synthesis of the mRNAs from the DNA controlled by regulatory elements called promoters. α defines transcription rate in the absence of the repressor (x). α indirectly depends on several factors, such as the abundance of the RNA polymerase and that of the repressilator plasmid in the cell. Therefore, this parameter may take very different values and we choose α as a bifurcation parameter, i.e. one to be varied. n is called Hill coefficient or cooperativity and reflects multimerization of the protein required to affect the promoter. Parameter Q reflects degree of the AI dilution in the medium. It is proportional to population density $\frac{V_{\text{cell}}}{V_{\text{medium}}}$ and can be varied from 0 (AI is strongly diluted) up to 1 (dense cell packing) [15]. The parameter β is a ratio between the decay rates of proteins and mRNAs. The three proteins are assumed to have identical kinetics, making the model symmetric.

The system and the scheme on Fig. 1 present a highly simplified model of the oscillatory network. In particular, intermediate reaction steps such as binding of an effector to a promoter are assumed to be very fast and, therefore, are not explicitly shown in the model. The system has been shown to oscillate both in experiments and in simulations for big enough α [7, 20, 21].

The simulations were performed by the numerical integration package XPP [22]. The numerical bifurcation analysis was done by AUTO [23] separately or in conjunction with the interface provided by XPP.

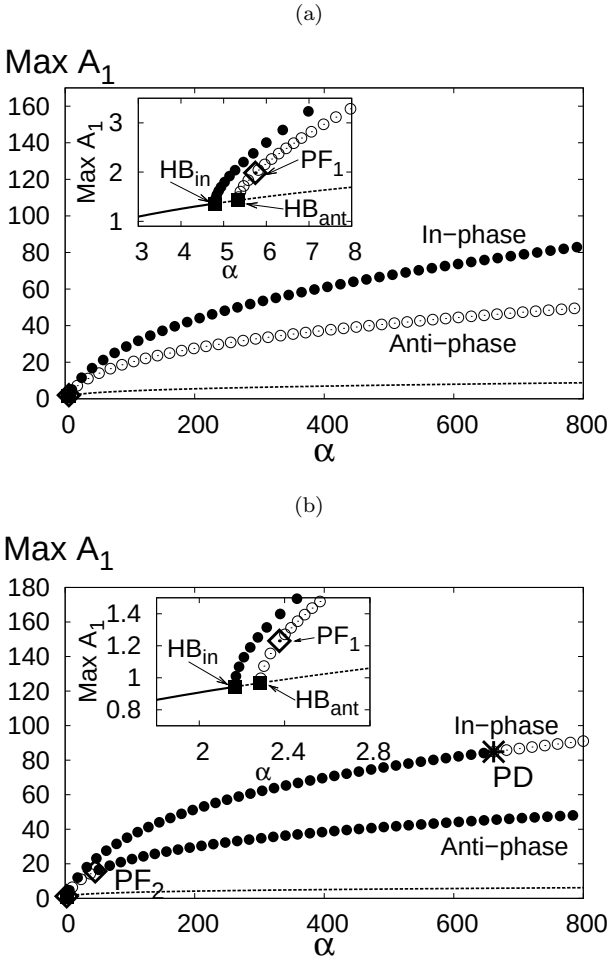

FIG. 2: The network switches from in- to anti-phase synchrony when the transcription cooperativity n is elevated. (a) $n = 2$, the in-phase limit cycle is stable; (b) $n = 2.6$, the in-phase cycle loses stability at higher values of α, the anti-phase one becomes stable as α increases. Solid (dashed) lines and solid (empty) circles denote stable (unstable) steady state and periodic solution, respectively. HB — Hopf, PF — pitchfork and PD — period doubling bifurcations. Parameters are: $\beta = 1.0$, $\kappa = 25.0$, $k_{s0} = 1.0$, $k_{s1} = 0.01$, $\eta = 2.0$, $Q = 1.0$ [15].

B. Anti-phase oscillations emerge at a higher cooperativity n

In-phase oscillations have been shown stable and robust in a model of a cell population bearing the repressilator plasmid with embedded system of quorum sensing [15]. An anti-phase synchronous solution must also exist, although its stability is a question. In the model cooperativity parameter $n = 2.0$ was used for all promoters. Later, a higher value around 2.4 was experimentally measured for one of those promoters, and the value was found to fluctuate dynamically [24]. Fig. 2(a) confirms the stability of the in-phase synchronization and shows

that the anti-phase synchronous solution is repelling at any synthesis rate α and $n = 2.0$.

Remarkably, the above picture is highly dependent on the cooperativity n. Higher values of n were numerically estimated for different promoters [25, 26]. If the cooperativity is elevated to 2.6 and further, the anti-phase solution becomes stable at a sufficiently high synthesis rate α (Fig. 2(b)). The solution becomes stable as a result of two sequential pitchfork bifurcations of limit cycles (PF_1 and PF_2) and remains stable when α increases further. By contrast, the in-phase solution loses its stability as α increases at this elevated n. All together, the synchronization properties are controlled by the parameters of the regulatory connections.

C. Fast mRNA kinetics provides birhythmicity in a wide range of α

We examine whether the ratio of mRNA and protein timescales β contributes to the synchronization properties. The ratio β is 1 in Fig. 2. This matches previous publications (e.g. [15]) and was achieved artificially by accelerating protein degradation [7]. Usually, protein kinetics, in particular degradation, is slower than that of mRNA ($\beta < 1$). It has been shown experimentally that lifetime of mRNA is of the order of 1 minute [27] while that of protein is about 1 hour [28]. Fig. 3 presents changes in the synchronous solutions as β is reduced towards more natural values. First, the sequence of the Hopf bifurcations changes: HB_{ant} occurs first now, and HB_{in} occurs next. Fig. 3(a) shows how the value α_{HB} for these two Hopf bifurcations depends on the ratio β. The bifurcation sequence changes at $\beta = 0.135$. Second, the stability of the limit cycles emerging at the Hopf bifurcations changes too. The anti-phase limit cycle, emerging first, (Fig 3(b), HB_{ant}) is initially stable. The in-phase limit cycle, emerging then, is unstable.

Three bifurcations always precede the birhythmic parameter regime when α increases. The in-phase solution must become stable. This occurs as a result of a repelling invariant torus emanating from the limit cycle (Fig. 3(b), TR_1). The other two bifurcations are unexpected: The anti-phase limit cycle first loses its stability, and then regains it. Both transitions are pitchfork bifurcations of limit cycles (Fig. 3(b)). The second bifurcation cancels the effect of the first one on the stability of the anti-phase solution. Thus, in an interval of the synthesis rate α, the anti-phase solution is unstable.

The pitchfork bifurcation PF_1 gives rise to a whole cascade of complex oscillatory solutions. One of them is a periodic solution different from the anti-phase by an amplitude mismatch between the cells (inhomogeneous anti-phase oscillations; Fig. 4(a)). Other complex dynamical regimes are shown in the Fig. 4(b),(c) and are not revealed by the bifurcation analysis (see Fig. 3(b)). More detailed analysis of the complex dynamical regimes is left for the future work.

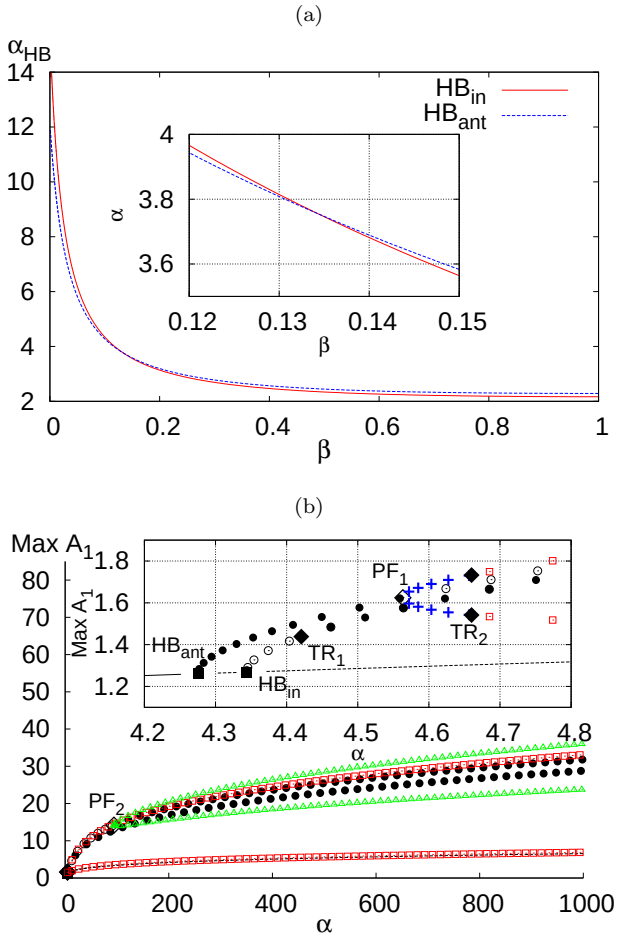

FIG. 3: (color online) A reduction in the timescale β provides birhythmicity in a wide range of α. (a) The sequence of the Hopf bifurcations changes when β passes the value of 0.135. (b) At $\beta = 0.1$ and $n = 2.6$, in-phase and anti-phase rhythms are stable at both moderate and high α. PF_1 gives rise to inhomogeneous anti-phase solutions — stable (blue crosses) and unstable (red squares), which are separated by a torus bifurcation (TR). PF_2 gives rise only to an unstable inhomogeneous anti-phase solution (green triangles). Other parameters and notations are the same as in Fig. 2(b).

Thus, there is an interval of moderate α where in-phase solution coexists with anti-phase and/or complex oscillatory solutions.

D. Discussion

In this work, we have presented a novel scenario of emerging birhythmicity and switching between the in-phase and anti-phase solutions in regulatory oscillators. The population can switch from in-phase to anti-phase synchronization when the transcription cooperativity is elevated. Stabilization of the anti-phase solution has

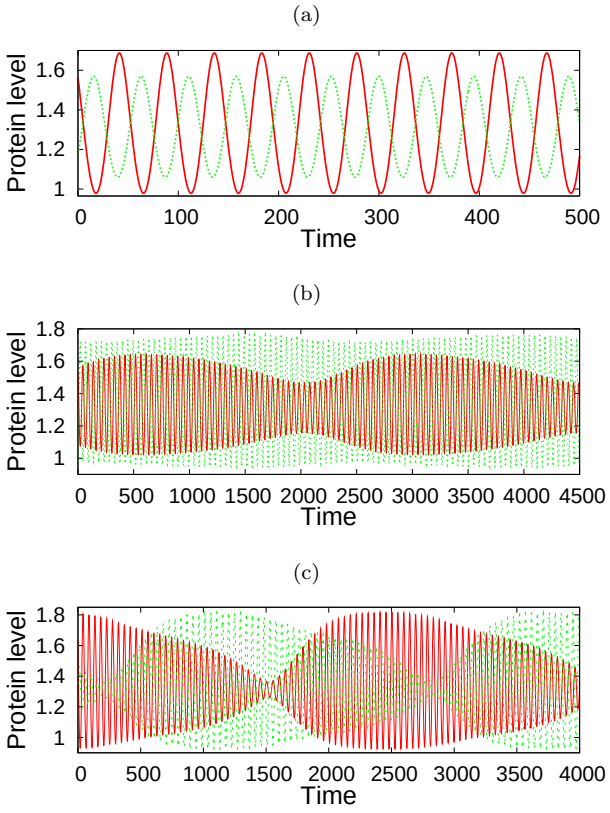

FIG. 4: (color online) Timeseries for complex anti-phase oscillations. A_1 is in red; A_2 is in green.$\beta = 0.1$ and other parameters are the same as in Fig. 2(b). (a) $\alpha = 4.60$; (b) $\alpha = 4.70$; (c) $\alpha = 4.75$.

been attributed to highly nonuniform motion speed along the oscillatory cycle [29]. There are two sources of such non-uniformity in the system analyzed here: First, the steepness of the nonlinear dependence (transcription cooperativity) translates into sadden acceleration and slowing. Second, increasing synthesis rate α in the repressilator leads to such a nonuniform motion as well [30]. Additionally, the population displays regimes where both stable in-phase and anti-phase rhythms coexist.

Many biophysical systems display certain properties found here. Stabilization of the anti-phase solution is consistent with other publications [29, 31–36]. The birhythmicity of the in-phase and the anti-phase oscillations is found in models of pancreatic β cells [37], yeast glycolysis [38], and coupled neural oscillators [31]. Recently, the anti-phase oscillations are shown to be stable in the repressilators with more complex, combinatorial regulation at the promoter level [39]. The question of general design principles governing synchronization properties remains open. Therefore, our results are related to a wide range of biophysical problems.

A central question in the analysis of regulatory networks is how to connect structural characteristics to dynamical and functional properties of a network. We have shown that the same network may display either in-phase or anti-phase synchronization, as well as the birhythmicity. Thus, the type of synchronization is not characteristic for the structure. The sequence in which the synchronous solutions emerge also depends on the parameters. However, the bifurcation scenario may be much more characteristic.

Variations of this bifurcation scenario were observed in a few works [31, 34, 38]. In [38] the first pitchfork bifurcation of the anti-phase solution is merged with the Hopf bifurcation, in which the solution emerges. In many other systems, the anti-phase solution becomes stable via a torus bifurcation (see e.g. [31]). These include a classical case of coupled Brusselators. In this paper, we never observe a torus bifurcation for the anti-phase solution. The anti-phase solution always undergoes two pitchfork bifurcations. This separates our results from those mentioned above.

Particular values of the synthesis rate α at the bifurcation transitions between the regimes depend on other parameters of the system. As we mentioned before, the transcription cooperativity n strongly influences bifurcations, not only quantitatively, but qualitatively changing parameter regimes. The parameters that influence synthesis of autoinducer (k_{s0},k_{s1}) also significantly shift the regimes, although bifurcation scenario does not change. Remarkably, the autoinducer dilution parameter Q does not shift the regimes in the parametric space much. Thus, our results are valid in a wide range of the population density. A thorough exploration of the parameter space for a larger population will be presented in a future work.

ACKNOWLEDGMENTS

I.P. and E.V. were supported by Russian Foundation of Basic Research grant 080200682. A.K. was supported by NSF grant DMS-0817717 and International Development Grant of Indiana University. We thank Dr. D. Zakharov for useful discussions.

[1] J. Dunlap, Cell **96**, 271 (1999).
[2] P. Nurse, Cell **100**, 71 (2000).
[3] A. Barion and P. Zee, Sleep Medicine **8**, 566 (2007).
[4] G. Evan and K. Vousden, Nature **411**, 342 (2001).
[5] M. Atkinson, M. Savageau, J. Myers, and A. Ninfa, Cell **113**, 597 (2003).
[6] T. Gardner, C. Cantor, and J. Collins, Nature **403**, 339 (2000).
[7] M. Elowitz and S. Leibler, Nature **403**, 335 (2000).
[8] A. Bekskei and L. Serrano, Nature **405**, 590 (2000).

[9] J. Hasty *et al.*, Chaos **11**, 207 (2001).
[10] B. Kholodenko, Nature Reviews **7**, 165 (2006).
[11] J. Tyson, K. Chen, and B. Novak, Nature Reviews **15**, 221 (2003).
[12] N. Barkai and S. Leibler, Nature **403**, 267 (2000).
[13] A. Kuznetsov, M. Kærn, and N. Kopell, SIAM Journal on Applied Mathematics **65**, 392 (2004).
[14] D. Yang, Y. Li, and A. Kuznetsov, Chaos **19** (2009).
[15] J. García-Ojalvo, M. Elowitz, and S. Strogatz, Proc. Natl. Acad. Sci. U.S.A. **101**, 10955 (2004).
[16] S. Yamaguchi *et al.*, Science **302**, 1408 (2003).
[17] D. McMillen, N. Kopell, J. Hasty, and J. J. Collins, Proc. Natl. Acad. Sci. U.S.A. **99**, 679 (2002).
[18] E. Ullner, A. Zaikin, E. I. Volkov, and J. Garcia-Ojalvo, Phys. Rev. Lett. **99**, 148103 (2007).
[19] T. Danino, O. Mondragón-Palomino, L. Tsimring, and J. Hasty, Nature **463**, 326 (2010).
[20] O. Buse, A. Kuznetsov, and R. Pérez, International Journal of Bifurcation and Chaos **19**, 4097 (2010).
[21] S. Müller *et al.*, J. Math. Biol. **53**, 905 (2006).
[22] B. Ermentrout, *Simulating, Analyzing and Animating Dynamical Systems: a Guide to XPPAUT for Researchers and Students*, 1st ed. (SIAM, 2002).
[23] E. Doedel, in *Cong. Num.*, Vol. 30 (Univ. of Manitoba, Winnipeg, Canada., 1981) pp. 265–284.
[24] N. Rosenfeld *et al.*, Science **307** (2005).
[25] S. Hooshangi, S. Thiberge, and R. Weiss, Proc. Natl. Acad. Sci. U.S.A. **102**, 3581 (2005).
[26] S. Zieser *et al.*, Theoretical Biology and Medical Modelling **3**, 11 (2006).
[27] J. Yu, J. Xiao, X. Ren, K. Lao, and X. Sunney Xie, Science **311**, 1600 (2006).
[28] J. Andersen *et al.*, Appl. Environ. Microbiol. **64**, 2240 (1998).
[29] D. Postnov, S. K. Han, and H. Kook, Phys. Rev. E **60**, 2799 (1999).
[30] O. Buse, R. Pérez, and A. Kuznetsov, Phys. Rev. E **81**, 066206 (2010).
[31] M. Kawato and R. Suzuki, J. Theor. Biol. **86**, 547 (1980).
[32] D. Aronson, G. Ermentrout, and N. Kopell, Physica D **41**, 403 (1990).
[33] E. Volkov and M. Stolyarov, Physics Letters A **159**, 61 (1991).
[34] G. Borisyuk, R. Borisyuk, A. Khibnik, and D. Roose, Bull. Math. Biol. **57**, 809 (1995).
[35] M. Rabinovich, R. Huerta, M. Bazhenov, A. K. Kozlov, and H. D. I. Abarbanel, Phys. Rev. E **58**, 6418 (1998).
[36] E. Izhikevich, SIAM J. Applied Mathematics **60**, 1789 (2000).
[37] D. Gonze, N. Markadieu, and A. Goldbeter, Chaos **18** (2008).
[38] J. Wolf and R. Heinrich, Biochem. J. **345**, 321 (2000).
[39] Yi, Q. Z., Zhang, J. J., Yuan, Z. J., and Zhou, T. S., Eur. Phys. J. B **75**, 365 (2010).